AIP | Applied Physics Letters

Micro rectennas: Brownian ratchets for thermal-energy harvesting

Y. Pan, C. V. Powell, A. M. Song, and C. Balocco

Citation: Applied Physics Letters **105**, 253901 (2014); doi: 10.1063/1.4905089
View online: http://dx.doi.org/10.1063/1.4905089
View Table of Contents: http://scitation.aip.org/content/aip/journal/apl/105/25?ver=pdfcov
Published by the AIP Publishing

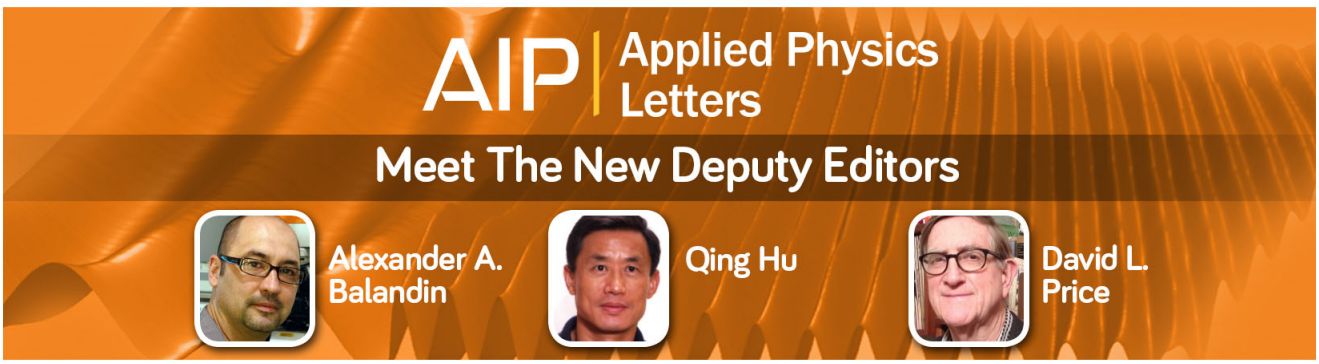

Micro rectennas: Brownian ratchets for thermal-energy harvesting

Y. Pan,[1] C. V. Powell,[1] A. M. Song,[2] and C. Balocco[1,a)]
[1]*School of Engineering and Computing Sciences, Durham University, Durham DH1 3LE, United Kingdom*
[2]*School of Electrical and Electronic Engineering, University of Manchester, Manchester M13 9PL, United Kingdom*

(Received 23 October 2014; accepted 15 December 2014; published online 23 December 2014)

We experimentally demonstrated the operation of a rectenna for harvesting thermal (blackbody) radiation and converting it into dc electric power. The device integrates an ultrafast rectifier, the self-switching nanodiode, with a wideband log-periodic spiral microantenna. The radiation from the thermal source drives the rectenna out of thermal equilibrium, permitting the rectification of the excess thermal fluctuations from the antenna. The power conversion efficiency increases with the source temperatures up to 0.02% at 973 K. The low efficiency is attributed mainly to the impedance mismatch between antenna and rectifier, and partially to the large field of view of the antenna. Our device not only opens a potential solution for harvesting thermal energy but also provides a platform for experimenting with Brownian ratchets. © *2014 AIP Publishing LLC*.
[http://dx.doi.org/10.1063/1.4905089]

Brownian ratchets are devices which generate useful work from random fluctuations. The devices have been increasingly studied for energy harvesting applications both through a theoretical[1] and experimental[2,3] approach. A classical model is Feynman's ratchet and pawl engine, which can extract useful mechanical work from Brownian motion from two heat baths at a different temperature.[4] The dissipative processes in electrical conductors result in thermal fluctuation, i.e., Johnson–Nyquist noise, and can be rectified to dc power by a diode if the system is brought out of thermal equilibrium. Feynman himself was the first to point out the similarities between the mechanical ratchet-and-pawl engine, and a diode driven by Johnson-Nyquist noise.[4] A more accurate model based on a master-equation approach was proposed and theoretically studied by Sokolov, consisting of a cold rectifier and a hot resistor.[5] A thermal rectenna consists of a high-speed rectifier coupled to an antenna, which collects the thermal radiation emitted by a blackbody source. If the temperatures of the rectifier and of the blackbody source are different, part of the random fluctuation on the rectifier can be converted to dc power. This device is conceptually similar to a rectifier connected to a resistor, and both systems can be essentially studied with the same model. The main difference is that, in the rectenna, the rectified dc power cannot be radiated (dissipated) by the antenna, whereas in the rectifier-resistor system the power is partially dissipated on the resistor, which limits the maximum theoretical efficiency even assuming no dissipation on the rectifier.[5]

The use of rectennas for energy harvesting was first proposed by Bailey[6] in 1972, for direct conversion of sunlight, and further developed by Mashaal and Gordon more recently.[7] However, challenges in the fabrication of high-speed rectifiers operating at optical frequencies, hundreds of terahertz, hampered the development. Moreover, most of the previous work on rectennas relies on coherent sources,[8,9] which neglect the important stochastic effects arising from the incoherent nature of the sources driving thermal rectennas.

In this letter, we demonstrate a micro-rectenna that is driven by thermal radiation to produce continuous electrical power. When illuminated by a hot body, the rectenna behaves as a thermal ratchet to harvest excess thermal fluctuations.[10] The system is brought to a non-equilibrium condition when the blackbody radiation collected by the antenna increases the antenna's effective temperature T_A rather than its physical one, above that of the rectifier T_D, which was maintained at room temperature. The antenna can be modelled as a resistor R_A at a temperature T_A, where R_A is the radiation resistance of the antenna.[11] An equivalent circuit diagram of the rectenna is shown in Fig. 1(a). The fictitious capacitor

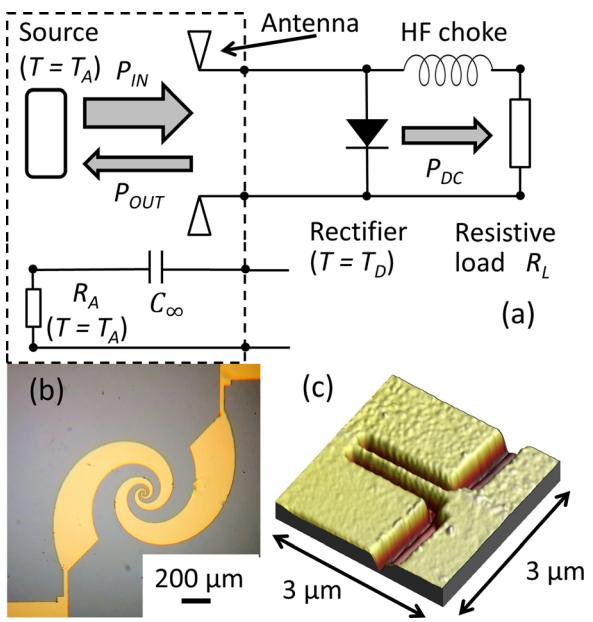

FIG. 1. (a) Schematic of the rectenna as an electronic ratchet. The dashed box shows the equivalent thermal resistor of the antenna illuminated by a source; (b) optical microscope image of the spiral antenna; and (c) atomic-force microscope (AFM) image of the SSD.

a)Author to whom correspondence should be addressed. Electronic mail: claudio.balocco@durham.ac.uk

C_∞ is introduced to account for the inability of the antenna to radiate a dc signal, thus decoupling the equivalent circuit into a time varying (ac) and a static (dc) sub-circuit. The dc power is delivered to the external load R_L through an inductor (consisting of the thin leads connecting the antenna arms to probing pads) which prevents (chokes) the radiation from leaking to the load.

As shown in Fig. 1(b), our rectenna consists of a wideband self-complementary log-periodic spiral antenna with a planar nanorectifier, a self-switching diode (SSD),[12,13] connected at the antenna feedpoint. The antenna was fabricated with a 200 nm thick layer of Au/Ge/Ni alloy. The spiral outer radius was approximately 600 μm and the centre gap is 5 ± 2 μm. The SSD was fabricated out of a two-dimensional electron gas (2DEG) embedded in a GaAs/AlGaAs quantum well 50 nm beneath the surface. The SSD consists of an asymmetric nano-channel, fabricated by etching two L-shaped trenches to insulate the 2DEG, as shown in Fig. 1(c). When a forward bias is applied, the positive potential on the channel sides provides a lateral field effect, which induces electrons within the channel, increasing its conductance and the current flow. On the other hand, the channel is laterally depleted when a reverse bias is applied and the current flow is consequently reduced. Hence, the structure behaves as an electric diode and the nonlinear current-voltage (*I-V*) characteristic is shown in the inset of Fig. 2. Details on the SSD fabrication, characterization can be found in Refs. 13 and 14. Theoretical models and numerical simulations are also available in the literature.[15–17]

The thermal radiation was generated by a temperature-controlled blackbody source with an emissivity above 0.99 and an output aperture diameter of 6.5 cm. An optical chopper was used with a 20 Hz reference for ease of measurement. The rectenna was placed immediately behind the chopper at a distance of 10 cm from the blackbody. The output voltage and current were read out by a lock-in amplifier. The device was mounted on a printed circuit board (PCB) maintained at room temperature (300 K). When illuminated by the thermal radiation, the rectenna generated a short-circuit current, I_{SC}, with a small current drop of within 10% of its peak value approximately 3 min after opening the blackbody-source shutter. This was ascribed to the thermal radiation heating up the rectenna slightly above room temperature, reducing the carrier mobility in 2DEG and thus the current.[18] Figure 2 plots I_{SC} as a function of the blackbody temperature T_0 from 573 K (300 °C) to 973 K (700 °C), the highest temperature permitted by the blackbody radiator. I_{SC} rose significantly with increasing T_0 and reached a value of approximately 6.6 nA at 973 K.

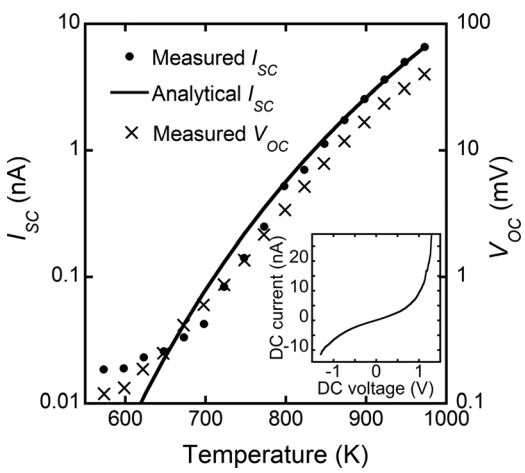

FIG. 2. I_{SC} and V_{OC} as a function of the blackbody temperature T_0; the inset shows the *I-V* characteristic of the rectenna measured at dc.

Following Feynman's approach, we described the rectification process using the analytical model of the ratchet and pawl engine[4,19]

$$I_D = I_0\left[\exp\left(-\frac{\phi - qV_D}{kT_A}\right) - \exp\left(\frac{-\phi}{kT_D}\right)\right], \qquad (1)$$

where I_D and V_D are the dc and voltage, respectively, across the rectifier, I_0 is an amplitude scaling factor with the dimension of a current, ϕ is a characteristic energy which can be identified with the diode built-in energy barrier, q is the elementary charge, and k is the Boltzmann's constant. The antenna and rectifier temperatures are T_A and T_D, respectively. As the blackbody did not fill the entire field of view of the antenna, is it safe to assume that the antenna temperature was lower than the blackbody temperature. Nevertheless, we made the conservative assumption that they were the same in the model and when calculating the conversion efficiency. Note that (1) reduces to the standard Shockley diode equation at equilibrium when $T_A = T_D$. When a short circuit is applied to the rectenna output, the rectified current I_D is the I_{SC}. A relatively good fit for the measured I_{SC} is obtained by setting ϕ as 0.94 eV and I_0 as 5.1 mA in the equation, as shown in Fig. 2. When an open circuit is present at the rectenna output, V_D is the open-circuit voltage, V_{OC}. Note that the voltage builds in the reverse bias region (as in the case of coherent radiation) if the $T_A > T_D$, but the model predicts a change in its sign should T_A be lower than T_D, Unfortunately, it was not possible to implement this experiment with our setup. The highest measured V_{OC} was 40 mV at 973 K. V_{OC} showed poor agreement with the analytical model because of the SSD reverse current, which made the *I-V* characteristic deviate from Shockley's diode equation. Assuming a linear *I-V* characteristic in the reverse bias explains why V_{OC} followed the shape of I_{SC}, as shown in Fig. 2, which could be ascribed to I_{SC} loading on the SSD differential resistance.

In order to quantify the harvested power, an external variable resistive load was connected in parallel to the rectenna. The current and voltage were measured as a function of the load resistance for a few different blackbody temperatures. The harvested power P_{DC} is given by $P_{DC} = V^2/R_L$, where V was the output voltage across the resistor of R_L. The ratio of the P_{DC} against the product of the V_{OC} and I_{SC} is used to find the fill factor (FF), which defines the maximum power point (MPP), as shown in Fig. 3. The measured fill factor was approximately 26% at the three temperature points considered. The value is consistent with our model. Assuming again a linear *I-V* characteristic in reverse bias, the MPP is found at $V_{OC}/2$ and $I_{SC}/2$, resulting in an expected fill factor of 25%. According to the basic circuit model, the optimal load R_L is equal to the resistance of the rectenna,

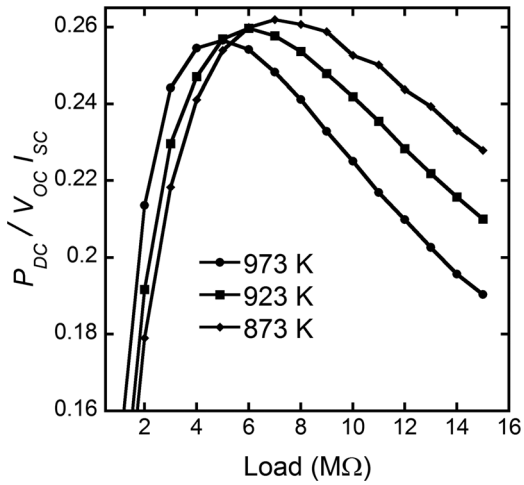

FIG. 3. The $P_{DC}/V_{OC}I_{SC}$ ratio as a function of the load resistance at three different temperatures; the peak value represents the rectenna fill factor.

showing a good agreement with the rectenna's dc resistances at corresponding temperatures which is obtained from the ratio of V_{OC} to I_{SC}.

Compared to the high conversion efficiency of coherent radiation (with a theoretical maximum of 100%), the thermal efficiency of a thermal rectenna or Brownian ratchet, in general, is strictly limited by the Carnot efficiency. Here, the efficiency η is defined as the output power on the load P_{DC} divided by the total available input power P_{AV}, $\eta(T) = P_{DC}/P_{AV}$. The thermal power can be calculated by multiplying the spectral radiation by Planck's law and the effective area of a receiving antenna, which is commonly given by $A_{eff} = \lambda^2/4\pi$, where λ is the radiation wavelength,[20] which results in the Johnson-Nyquist power spectral density[11]

$$S(T;\nu) = kT\frac{h\nu/kT}{\exp(h\nu/kT) - 1}, \tag{2}$$

where h is Planck's constant, k is the Boltzmann's constant, and T is the body temperature. Equivalently, the diode at the temperature T_D also emits radiation, with the same power spectral density $S(T_D;\nu)$. Figure 4(a) shows the calculated power spectral densities of the antenna at $T_A = 973$ K and the diode at $T_D = 300$ K, which are relatively flat for frequencies below the quantum cut-off. The dashed line marks the quantum cut-off frequencies where $h\nu/kT = 1$. Integrating over all frequencies, the available power is

$$P_{AV} = (\sigma\pi^2/6h) \times [(kT_A)^2 - (kT_D)^2], \tag{3}$$

where σ is the emissivity of 0.99 for the blackbody.[11] The rectenna efficiency is plotted in Fig. 4(b), which rises by almost five orders of magnitude over the temperature range of 400 K. The maximum efficiency reaches 0.02% at 973 K, which is still far lower than the Carnot efficiency.[21]

The low efficiency is ascribed to the impedance mismatch between the antenna and the diode, which resulted in very high power reflection, by the antenna field of view to the blackbody, and by the frequency response of the antenna. The main cause of the low efficiency, however, is the impedance mismatch; the dc resistance of the rectenna obtained from the measurement was almost flat at 8.5 MΩ below

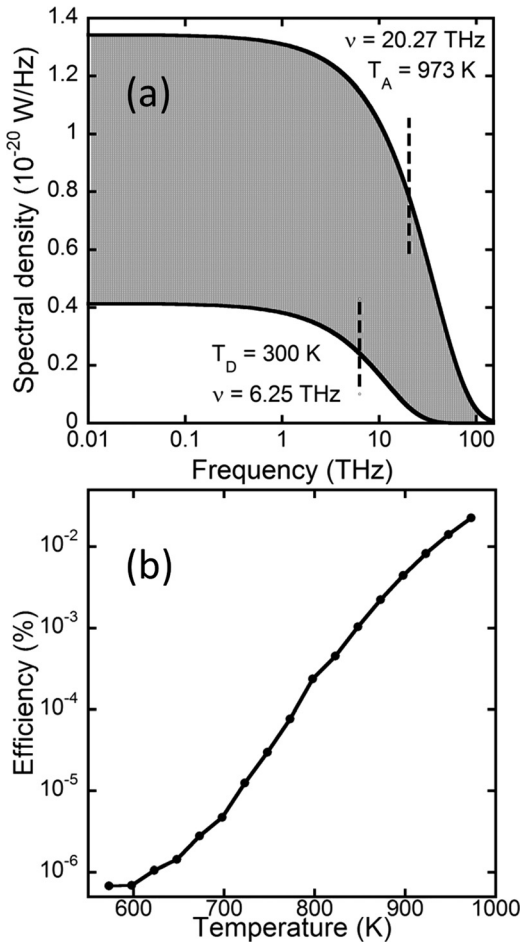

FIG. 4. (a) The spectral densities at $T_A = 973$ K and $T_D = 300$ K. The available power for the rectification is the grey-filled area. (b) The power conversion efficiency η as a function of the blackbody temperature.

800 K, decreasing linearly to 6 MΩ at 973 K, mainly because of the diode's nonlinear I-V characteristic. Numerical simulations (performed with Agilent Advanced Design System, ADS) gave an average antenna impedance of approximately 80 Ω in the frequency range of interest, with a negligible imaginary part (as expected by the self-complementary geometry), resulting in a transmission coefficient from the antenna to the diode of the order of 10^{-5}–10^{-6} if the dc resistance is used. However, the actual reflection coefficient is expected to be higher than this value due to the reactive components of the SSD, which are difficult to characterize at THz frequencies. The effective antenna temperature was also lower than the blackbody temperature because the antenna saw a large amount of radiations from cold surroundings apart from the blackbody. The strong temperature dependence of the efficiency is due to the exponential dependence of the current and voltage as a function of the temperature when the rectenna operates at its maximum power point, and it is well described by Eq. (1). The voltage which builds across the rectifier is in first approximation proportional to the current through the parallel resistance. The exponential temperature dependence observed in the current (as shown in Fig. 2) is thus emphasized in the power, which ultimately results in the dependence observed in Fig. 4.

Figure 5 shows the receiving pattern of the spiral antenna. The normalized rectified output power has a maximum at the

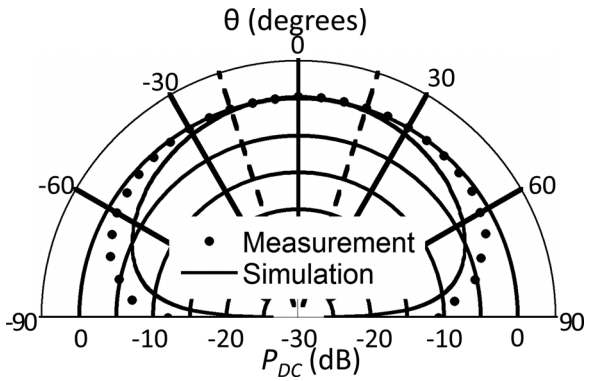

FIG. 5. Measured and simulated receiving pattern of the spiral rectenna. The dashed lines delimit the field of view covering the finite blackbody source.

normal incidence as $\theta = 0$ as expected. While the simulations were performed assuming a perfect conductor for the spiral and a lossless GaAs substrate, the results show a good agreement with the measurement in Fig. 5. The measured half-power beam width is approximately 140°. The field of the view of the rectenna to the blackbody is approximately 36° as highlighted by the red dashed lines in the figure. It is thus clear that the efficiency would also be improved by increasing the field of view to the blackbody.

The frequency response of the rectenna was estimated by using high-pass optical mesh filters. The filters were fabricated on a 50 μm thick copper shim with periodical square arrays of rectangular holes. The frequency components can pass through low attenuation when $f > c/p$, where c is the speed of light in vacuum and p is the pitch of the square hole.[22] Filter A had a 150 μm pitch and a 100 μm side length of the square hole, while filter B has a 100 μm pitch and a 50 μm side length. The filter corner frequencies were approximately 2.0 and 3.0 THz for filters A and B, respectively. We observed that the short-circuit currents with filters A and B dropped to 77% and 62% of the I_{SC} with no filters at 973 K, respectively. This implies that the majority of dc power is rectified over the higher THz frequencies. The upper frequency limit is mostly determined by the inner diameter of the spiral antenna, as $f_c = c/(\pi d\sqrt{\varepsilon})$,[19] where the nominal diameter of d is 5 μm and the GaAs substrate permittivity ε is 12.8. Thus, f_c is approximately 5.3 THz. The cut-off frequency is below the optical phonon absorption of the GaAs substrate at approximately 8.1 THz,[23] which sets the fundamental upper frequency limit for the power when using GaAs substrate.

In summary, we demonstrated a thermal rectenna which converts thermal radiation from a blackbody source to dc electric power. However, even by improving the conversion efficiency, the maximum output power from a single rectenna would be too low to be used in practical applications. The overall power extraction can be improved to a useful level by implementing an array of rectennas. The finite size of an antenna determines the lower cut-off frequency, but enables a larger number of antennas on the same substrate area. Preliminary numerical results show that the rectified power from a single element drops with the shorter antenna length as expected, and that by increasing the total number of rectennas per unit area the power increases up to a certain point, where the central frequency of the antenna is of the order of the quantum cut-off frequency. Our current works currently focus on testing the efficiency of these large arrays and study their efficiency as a function of the antenna geometry.

We wish to thank Dr. Zheng Kuang for manufacturing the THz filters. We acknowledge financial support from EPSRC, Grant No. EP/K016857/1 and from EU FP7 ITN NOTEDEV, Grant No. 607521.

[1]P. Reimann, Phys. Rep. **361**, 57 (2002).
[2]E. M. Roeling, W. C. Germs, B. Smalbrugge, E. J. Geluk, T. de Vries, R. A. Janssen, and M. Kemerink, Nat. Mater. **10**, 51 (2011).
[3]P. Olbrich, E. Ivchenko, R. Ravash, T. Feil, S. Danilov, J. Allerdings, D. Weiss, D. Schuh, W. Wegscheider, and S. Ganichev, Phys. Rev. Lett. **103**, 090603 (2009).
[4]R. P. Feynman, R. B. Leighton, and M. L. Sands, *The Feynman Lectures on Physics: Mainly Mechanics, Radiation, and Heat* (Addison-Wesley, Reading, MA, 1966), Vol. I.
[5]I. Sokolov, Europhys. Lett. **44**, 278 (1998).
[6]R. L. Bailey, J. Eng. Gas Turbines Power **94**, 73 (1972).
[7]H. Mashaal and J. M. Gordon, Opt. Lett. **36**, 900 (2011).
[8]J. A. Hagerty, F. B. Helmbrecht, W. H. McCalpin, R. Zane, and Z. B. Popovic, IEEE Trans. Microwave Theory **52**, 1014 (2004).
[9]F. M. Congedo, G. Monti, L. Tarricone, and M. Cannarile, in *Proceedings of the 5th European Conference on Antennas and Propagation, EuCAP* (2011), pp. 335–3375.
[10]A. De Vos, *Thermodynamics of Solar Energy Conversion* (Wiley-Vch, Berlin, 2008).
[11]B. M. Oliver, Proc. IEEE **53**, 436 (1965).
[12]C. Balocco, A. Song, M. Åberg, A. Forchel, T. González, J. Mateos, I. Maximov, M. Missous, A. Rezazadeh, and J. Saijets, Nano Lett. **5**, 1423 (2005).
[13]C. Balocco, S. R. Kasjoo, X. F. Lu, L. Q. Zhang, Y. Alimi, S. Winnerl, and A. M. Song, Appl. Phys. Lett. **98**, 223501 (2011).
[14]C. Balocco, M. Halsall, N. Vinh, and A. Song, J. Phys.: Condens. Matter **20**, 384203 (2008).
[15]P. Sangaré, G. Ducournau, B. Grimbert, V. Brandli, M. Faucher, C. Gaquière, A. Íñiguez-de-la-Torre, I. Íñiguez-de-la-Torre, J. F. Millithaler, and J. Mateos, J. Appl. Phys. **113**, 034305 (2013).
[16]I. Iñiguez-de-La-Torre, J. Mateos, D. Pardo, and T. González, J. Appl. Phys. **103**, 024502 (2008).
[17]J. Mateos, B. Vasallo, D. Pardo, and T. González, Appl. Phys. Lett. **86**, 212103 (2005).
[18]G. Ng, D. Pavlidis, M. Quillec, Y. Chan, M. Jaffe, and J. Singh, Appl. Phys. Lett. **52**, 728 (1988).
[19]J. M. Parrondo and P. Español, Am. J. Phys. **64**, 1125 (1996).
[20]F. González and G. Boreman, Infrared Phys. Technol. **46**, 418 (2005).
[21]P. Landsberg and P. Baruch, J. Phys. A: Math. Gen. **22**, 1911 (1989).
[22]R. Ulrich, Infrared Phys. **7**, 37 (1967).
[23]E. D. Palik, *Handbook of Optical Constants of Solids* (Academic, New York, 1998), Vol. III.